Earth Syst. Sci. Data Discuss., https://doi.org/10.5194/essd-2017-46
Manuscript under review for journal Earth Syst. Sci. Data
Discussion started: 15 June 2017

Pages without corrections are omitted

Altimetry, gravimetry, GPS and viscoelastic modelling data for the joint inversion for glacial isostatic adjustment in Antarctica (ESA STSE Project REGINA)

Ingo Sasgen[1], Alba Martín-Español[2], Alexander Horvath[3], Volker Klemann[4], Elizabeth J. Petrie[5], Bert Wouters[6], Martin Horwath[7], Roland Pail[3], Jonathan L. Bamber[2], Peter J. Clarke[8], Hannes Konrad[9], Terry Wilson[10] and Mark R. Drinkwater[11]

1. Division of Climate Sciences, Alfred Wegener Institute, Bussestraße 24, 27570 Bremerhaven, Germany.
2. School of Geographical Sciences, University of Bristol, University Road, Clifton, Bristol BS8 1SS, United Kingdom.
3. Institut für Astronomische und Physikalische Geodäsie, Technische Universität München, Arcisstraße 21, 80333 München, Germany.
4. Department of Geodesy, GFZ German Research Centre for Geosciences, Telegrafenberg, 14473 Potsdam, Germany.
5. School of Geographical and Earth Sciences, University of Glasgow, Glasgow, G12 8QQ, United Kingdom.
6. Institute for Marine and Atmospheric Research, Utrecht University, Princetonplein 5, 3584 CC, Utrecht, The Netherlands.
7. Institut für Planetare Geodäsie, Technische Universität Dresden, Helmholtzstr. 10, 01069 Dresden, Germany.
8. School of Civil Engineering and Geosciences, Newcastle University, Newcastle, NE1 7RU, United Kingdom.

Earth Syst. Sci. Data Discuss., https://doi.org/10.5194/essd-2017-46
Manuscript under review for journal Earth Syst. Sci. Data
Discussion started: 15 June 2017

Earth System Science Data
Open Access Discussions

ABSTRACT

A major uncertainty in determining the mass balance of the Antarctic ice sheet from measurements of satellite gravimetry, and to a lesser extent satellite altimetry, is the poorly known correction for the ongoing deformation of the solid Earth caused by glacial isostatic adjustment (GIA). In the past decade, much progress has been made in consistently modelling the ice sheet and solid Earth interactions; however, forward-modelling solutions of GIA in Antarctica remain uncertain due to the sparsity of constraints on the ice sheet evolution, as well as the Earth's rheological properties. An alternative approach towards estimating GIA is the joint inversion of multiple satellite data – namely, satellite gravimetry, satellite altimetry and GPS, which reflect, with different sensitivities, trends of recent glacial changes and GIA. Crucial to the success of this approach is the accuracy of the space-geodetic data sets. Here, we present reprocessed rates of surface-ice elevation change (Envisat/ICESat; 2003-2009), gravity field change (GRACE; 2003-2009) and bedrock uplift (GPS; 1995-2013.7). The data analysis is complemented by the forward-modelling of viscoelastic response functions to disc load forcing, allowing us to relate GIA-induced surface displacements with gravity changes for different rheological parameters of the solid Earth. The data and modelling results presented here are available in the Pangeae archive; https://doi.pangaea.de/10.1594/PANGAEA.875745. The data sets are the input streams for the joint inversion estimate of present-day ice-mass change and GIA, focusing on Antarctica. However, the methods, code and data provided in this paper are applicable to solve other problems, such as volume balances of the Antarctic ice sheet, or to other geographical regions, in the case of the viscoelastic response functions. This paper presents the first of two contributions summarizing the work carried out within a European Space Agency funded study, REGINA.

Earth Syst. Sci. Data Discuss., https://doi.org/10.5194/essd-2017-46
Manuscript under review for journal Earth Syst. Sci. Data
Discussion started: 15 June 2017

Earth System Science Data
Open Access Discussions

1. Introduction

Glacial isostatic adjustment (GIA), the viscoelastic deformation of the solid Earth in response to climate-driven ice and water mass redistribution on its surface, is poorly constrained in Antarctica. The primary reason is the sparseness of geological evidence of the past ice sheet geometry and local relative sea-level change. These are important constraints on the exerted glacial forcing and on the viscoelastic structure of the lithosphere and of the mantle, respectively, which concertedly determine the signature of GIA (e.g. Peltier, 2004; Ivins and James 2005; Whitehouse et al. 2012: van der Wal et al., 2015). The predictions of GIA in Antarctica remain ambiguous (Shepherd et al. 2012, suppl.) and cause a large uncertainty in gravimetric mass balance estimates of the ice sheet of the order of the estimate itself (Martín-Español et al. 2016b). Measurements of bedrock uplift by GPS have shown to be inconsistent with forward models, which tend to over-predict uplift and mass increase due to GIA, biasing estimates of present-day Antarctic ice-mass loss from GRACE to more negative values (Bevis et al. 2009).

Much progress has been made in reconstructing the ice sheet evolution from geomorphological evidence (Bentley et al. 2014) and inferring the underlying Earth structure from seismic observations (An et al. 2015; Heeszel et al. 2016). However, an independent approach to constraining GIA is to make use of the different sensitivities of the various types of satellite data to recent glacial changes and GIA, respectively. And thus to separate both signals in a joint inversion approach has been pursued by e.g. Wahr et al. 2000; Riva et al. 2009; Wu et al. 2010; Gunter et al. 2014, Martín-Español et al. 2016a. Another approach used regional patterns of GIA from forward modelling and adjusted them to GIA uplift rates in Antarctica (Sasgen et al. 2013).

Earth Syst. Sci. Data Discuss., https://doi.org/10.5194/essd-2017-46
Manuscript under review for journal Earth Syst. Sci. Data
Discussion started: 15 June 2017

Open Access Earth System Science Data Discussions

In this paper, we present methods and data inputs in preparation of solving the joint inversion for GIA in Antarctica. As the GIA process is gradual, causing an approximately constant rate of change within a decade, we first process the satellite data to recover optimal temporal linear trends. We refine existing procedures for the surface-ice elevation changes from Envisat and ICESat satellite altimetry (Section 2), bedrock displacement from *in situ* networks of GPS stations in Antarctica (Section 3), and gravity field change from GRACE (Section 4). We also present forward modelling results of viscoelastic response functions to disc load forcing for the range of Earth structures likely to prevail in Antarctica (Section 5).

The determination of viscoelastic response functions is a classic topic in solid Earth modelling (e.g. Peltier & Andrews, 1976), though uncommon the application to joint ~~invasion~~ studies of satellite data. Although this paper focusses on Antarctica, the response functions and data processing techniques presented here are applicable to other regions. The response kernels represent a wide range of Earth structures and can be used for the separation of superimposed present-day (elastic) and past (viscoelastic) signatures of mass change in other regions, for example hydrological storage changes and GIA in North America. The response functions give insight into the temporal and spatial scales of deformation expected for Antarctica, and are crucial when combining the input data streams.

The data sets and modelling results presented in this paper are accessible in the Pangeae archive, https://www.pangaea.de/ – subsections provide user guidance and point to data and code stored in the archive. As mentioned above, the data sets and modelling results are of value to address other research questions as well. For example, the GPS rates provided are useful for the validation of forward modelling GIA solutions, the GRACE gravity rates can be used for mass balance studies, and altimetry data 2003-2009 can be extended with the ongoing CryoSat-

Earth Syst. Sci. Data Discuss., https://doi.org/10.5194/essd-2017-46
Manuscript under review for journal Earth Syst. Sci. Data
Discussion started: 15 June 2017

Earth System Science Data
Open Access Discussions

2 mission to infer volumetric mass balances, also over the ice shelves. The viscoelastic response functions are based on Earth model parameters potentially suitable to other geographical regions, as well;
111 they are useful for similar studies combining different data sets of geodetic observables, surface deformation, gravity field change, and topographic change in glaciated areas.

The actual method of the joint inversion is described in a second contribution of the
114 REGINA project team (Sasgen et al. *submitted*). In ~~this~~ that second paper, the resulting GIA estimate is also compared to previous studies. The processing of the data issued here was enabled by the European Space Agency within the CryoSat+ Support To Science Element Study REGINA.
117

Explain why 2003-2009 was chosen for ~~GRACE~~ but a longer time span for GNSS.

~~Hint~~ Emphasize key assumption of constant rate over 1995–2013

Earth Syst. Sci. Data Discuss., https://doi.org/10.5194/essd-2017-46
Manuscript under review for journal Earth Syst. Sci. Data
Discussion started: 15 June 2017

Open Access Earth System Science Data Discussions

2. ALTIMETRY DATA ANALYSIS

2.1 *ICESat elevation rate determination*

We use along-track altimetry measurements from *ICESat 633 Level 2*, providing high-resolution elevation change observations for the period February 2003 until October 2009. Two corrections are applied to this data set: the range determination from Transmit-Pulse Reference-Point Selection (Centroid vs. Gaussian) (Borsa et al. 2014) available from the National Snow and Ice Data Center (NSIDC), and the inter-campaign correction (Hofton et al. 2013). The Centroid-Gaussian correction is a well-established correction and has been incorporated to the latest ICESat release (634). Concerning the ICESat Intercampaign Bias (ICB) correction, uncertainties are available at Hofton et al (2013). Furthermore, several studies have determined this correction from different methodologies. For a summary of published ICESat ICB corrections see Scambos & Shumman (2016). Because ICESat tracks do not usually overlap, a regression approach is used in which topographic slope (both across-track and along-track) and the rate of surface-elevation change $\boldsymbol{y}^{h}_{\mathrm{ICESat}}$, are simultaneously estimated using the 'plane' method (Howat et al. 2008) over areas spanning 700 m long and few hundred meters wide. A regression is only performed if a plane has at least 10 points from four different tracks that span at least one year. Regression was carried out twice; first, individual elevation measurements with corresponding residuals outside the range of two standard deviations were detected, then, the regression was repeated omitting these outliers. The standard deviation of the regression coefficient, here taken as the uncertainty of the elevation rate, σ^{h}(here, ICESat) is calculated by the propagation of the residual uncertainties of the topographic heights,

$$\hat{s}_{\mathrm{ICESat}} = \sqrt{\frac{\sum e_i^2 / (n-2)}{\sum (x_i - \bar{x})^2}}, \quad (1)$$

Earth Syst. Sci. Data Discuss., https://doi.org/10.5194/essd-2017-46
Manuscript under review for journal Earth Syst. Sci. Data
Discussion started: 15 June 2017

Earth System Science Data
Open Access Discussions

to the trend parameter, where $\boldsymbol{e}$ is the vector of residuals, n is the sample size ($i = 1,2, \ldots, n$), and $\boldsymbol{x}$ is the vector of input elevations with mean $\bar{x}$. This standard deviation (σ_{ICESat}) takes into account the sample size and the variance of both input data and residuals of the regression (Hurkmans et al. 2012). The exact ICESat observation periods are shown in the Appendix (A.1, Table A.1). Then, the elevation rate and its uncertainty are interpolated to a common 10 × 10 km grid in polar-stereographic projection (central latitude 71°S; central longitude 0°W, and origin at the South Pole, WGS-84 reference ellipsoid).

2.2 *Envisat elevation rate determination*

We use a time series of elevation changes derived from along-track Envisat radar altimetry data for the interval January 2003 to October 2009 (coeval to ICESat time span). Elevation rates y^{h}_{Envisat} are obtained at points every 1 km along track, by binning all the echoes within a 500 m radius. Then, a 10-parameter least squares model is fitted in order to correct for the across-track topography and changes in snowpack properties. The least square model is defined in Flament and Remy (2012). The estimated parameters include parameters determined for the backscatter, leading-edge width and tailing-edge slope, the mean altitude, quadratic surface slope parameters to define surface curvature and a linear time trend. A digital elevation model was not used for the correction of the topographic slope. For processing reasons, the temporal resolution is re-sampled from 35 days to monthly periods for each grid cell, before estimating the elevation rates. This has a minor effect on the elevation rate estimate (smaller than ± 1 cm) and reduces the standard deviation by about 14 %. As for ICESat, the elevation rate is interpolated to a common 10 × 10 km polar stereographic grid, and the standard deviations of the rates within each grid cell are taken as an estimate of the measurement uncertainty, $\sigma_{\mathrm{Envisat}}$.

units? mismatch

with

Earth Syst. Sci. Data Discuss., https://doi.org/10.5194/essd-2017-46
Manuscript under review for journal Earth Syst. Sci. Data
Discussion started: 15 June 2017

Earth System Science Data
Open Access Discussions

86°S for ICESat due to satellite orbit inclination. On the Antarctic Peninsula, Envisat picks up some points that are not present due to a sparser track coverage in the ICESat data set. As expected, ICESat outperforms Envisat in terms of uncertainty of the elevation rate over steep topographic slopes and along the ice sheet margins. This is due to the smaller footprint of the laser altimeter, its higher accuracy and lower slope-dependent uncertainty (e.g. Brenner 2007). On some flat areas and over some faulty ground tracks, where ICESat data measurements are scarce, however, Envisat provides better temporal and spatial coverage leading to better accuracy of the resulting elevation rates. The resulting combined data set of surface-elevation rates and its uncertainties are shown in Fig. 2.

Can you present $\frac{(data\_used - data\_not\_used)}{\sigma_{ice}^2 + \sigma_{emi}^2}$?

Or summarize statistics?

Why this instead of weighted average?

Earth Syst. Sci. Data Discuss., https://doi.org/10.5194/essd-2017-46
Manuscript under review for journal Earth Syst. Sci. Data
Discussion started: 15 June 2017

Open Access Earth System Science Data Discussions

183 2.4 *Firn correction*

The elevation rates derived from ICESat and Envisat are corrected for changes in the firn layer thickness using the firn compaction model of Ligtenberg (2011), which is driven by the
186 regional atmosphere and climate model RACMO2/ANT (Lenaerts, 2010). We determine the firn compaction for January 2003 to October 2009, with respect to the mean of the years 1979 to 2002 and estimate a temporal linear trend, h_{comp}. The model output is re-gridded onto the
189 10×10 km common grid using nearest neighbor interpolation. The standard deviation of the re-gridding is less than 1 cm/yr, causing a maximum change of 2 % of the firn compaction rate. Note that the firn compaction model has a spatial resolution of 27 km, potentially neglecting
192 finer-scale processes relevant for the altimetry data. Clearly, the re-gridding uncertainty stated above is merely a minimum estimate, neglecting, for example, uncertainties in the calibration or the atmospheric forcing of the firn compaction model.

195 The data were re-sampled from every two days to monthly mean time periods for every grid cell before estimating elevation rates. As for the Envisat and ICESat data, no seasonal terms are co-estimated and removed (i.e. annual and semi-annual). We do not apply an *a priori*
198 correction for surface-mass balance (SMB) trends, in accordance with the GRACE processing (Section 5), which requires defining a climatological reference period. Note that applying the commonly used reference period (1979 to present) leads to spurious accumulation anomalies
201 in the altimetry data (see Appendix A.2, Fig. A.1). The derivation of an adequate climatological reference epoch in the RACMO2/ANT simulations is in itself challenging and beyond the scope of this paper.

204 The total uncertainty of the rate of elevation change from satellite altimetry is calculated by

Earth Syst. Sci. Data Discuss., https://doi.org/10.5194/essd-2017-46
Manuscript under review for journal Earth Syst. Sci. Data
Discussion started: 15 June 2017

Open Access Earth System Science Data Discussions

Explain re-sampling from 27 km grid to 10 km grid

$$\sigma_h = \sqrt{\sigma^2_{\text{Envisat/ICESat}} + \sigma^2_{\text{Firn}}}, (2)$$

where the standard deviation of the firn correction, σ_{Firn} is the formal regression uncertainty (neglecting model uncertainties, as these are not available), and we assume the error sources to be uncorrelated.

2.5 *Data availability*

Not a complete sentence — no verb

Annual elevation trends from a combination of Envisat and ICESat data for the time period between February 2003 and October 2009. Trends have been corrected for firn densification processes using RACMO2/ANT. Elevation trends are provided in a 20 km polar stereographic grid (central meridian 0◦ , standard parallel 71◦ S) with respect to the WGS84 geoid. X and Y are given in km, and the elevation rate and its standard deviation are given in m/yr.

relationship to 10 x 10 grid? decimated? averaged? block median?

2.5.1 *ICESat elevation trend for the* time period between February 2003 and October 2009.

The dataset is provided in a 10 km grid in polar stereographic projection (central meridian 0◦da standard parallel 71◦ S) with respect to the WGS84 geoid. X and Y are given in km, and the elevation rate and its standard deviation are given in m/yr.

2.5.2 *Envisat elevation trend for the time period between February 2003 and October 2009.*

The dataset is provided in a 10 km grid in polar stereographic projection (central meridian 0◦ , standard parallel 71◦ S) with respect to the WGS84 geoid. X and Y are given in km, and the elevation rate and its standard deviation are given in m/yr.

Earth Syst. Sci. Data Discuss., https://doi.org/10.5194/essd-2017-46
Manuscript under review for journal Earth Syst. Sci. Data
Discussion started: 15 June 2017

Open Access Earth System Science Data Discussions

2.5.3 ICESat & Envisat combination for time period between February 2003 and October 2009.

define acronym or just spell it out

Elevation changes have been corrected for firn densification processes using a FDM. The dataset is provided in a 10 km grid in polar stereographic projection (central meridian 0° to standard parallel 71° S) with respect to the WGS84 geoid. X and Y are given in km, and the elevation rate and its standard deviation are given in m/yr.

2.5.4 *Annual elevation trends from CryoSat-2 derived from a single trend covering the time period 2010-2013.*

An acceleration term in areas with dynamic thinning was added to the linear trend to obtain annual rates. Elevation trends are provided at 10 km resolution in a polar stereographic grid (central meridian 0° , standard parallel 71° S) with respect to the WGS84 geoid. X and Y are given in km and the elevation rate and its standard deviation are given in m/yr.

2.5.5 *Elevation changes from firn model*

Annual firn densification rates over 2003-2013 rates obtained from RACMO2.3. Data is provided in a 27 km polar stereographic grid (central meridian 0° , standard parallel 71° S) with respect to the WGS84 geoid. X and Y are given in km and the annual firn densification rates in m/yr.

2.5.6 *Snow / ice density map*

The density map for volume-to-mass conversion is provided in 20 km resolution in a polar stereographic grid (central meridian 0° , standard parallel 71° S) with respect to the WGS84 geoid. X and Y are given in km and density in km/m^3.

2.5.7 *ICESat/Envisat combination mask*

Mask used for combining ICESat and Envisat in a 10 km resolution and polar stereographic

Earth Syst. Sci. Data Discuss., https://doi.org/10.5194/essd-2017-46
Manuscript under review for journal Earth Syst. Sci. Data
Discussion started: 15 June 2017

Earth System Science Data Discussions

249 coordinates.

X and Y are coordinates in km and the id represents whether ICESat or Envisat has been used to construct the elevation change combination.

252 4: only Envisat was available

3: only ICESat was available

2: ICESat lower errors

255 1: Envisat lower errors

3. GPS UPLIFT RATE ESTIMATION & CLUSTERING

The aim of the GPS time series analysis is to derive uplift rates, y_u that represent the vertical
258 ~~geophysical~~ ground motion at the sites as accurately and robustly as possible. We derive uplift rates based on GPS records from a total of 118 Antarctic sites. Data were processed from 1995 day of year (doy) 002 to 2013 doy 257 (1995.0-2013.7) but data at individual sites are of varying
261 length and quality. The processing and uplift rate and uncertainty estimation methodology are documented in detail in Petrie et al. (in prep. a, b), but a short summary is given here for convenience. It resembles that of Thomas et al. (2011), but with more recent processing
264 software (GIPSY 6.2) and model updates (including second order ionospheric and earth radiation models): an initial satellite orbit and clock estimation step is performed, using a carefully selected balanced stable global network of GPS sites. The orbits and clocks are then
267 used to perform precise point positioning (PPP) processing of all the available Antarctic sites of interest. A mini-ensemble was created to investigate systematic processing uncertainties and ~~manual investigation was performed of~~ the effects of effects of possible systematic errors in the time series
270 on uplift rates. The mini-ensemble investigation showed that decisions taken when analyzing time series tended to have larger effects on uplift rates and uncertainties than the effects of small

why not just use JPL's orbits and clocks? A 1-sentence reason is adequate (presumably to ensure consistency)

position was investigated using this mini-ensemble

Earth Syst. Sci. Data Discuss., https://doi.org/10.5194/essd-2017-46
Manuscript under review for journal Earth Syst. Sci. Data
Discussion started: 15 June 2017

Earth System Science Data
Open Access Discussions

processing strategy changes. Outliers and systematic errors, such as offsets due to equipment changes or other causes, were removed where possible. Due to the varying characteristics of the time series it was not possible to use the same approach at all sites. The strategy was as follows (and is summarized in Appendix A.3, Fig. A.3). For sites with over 2000 days of data, uplift rates and associated uncertainties were estimated using the CATS software (Williams 2008). We co-estimated a white-noise scale factor for the formal uncertainties, and a power-law noise amplitude with the index fixed to -1 (flicker noise), along with the temporal linear trend (rate), seasonal (annual and semi-annual) parameters, and sizes of the offsets (at the specified epochs).

The median values of the white-noise scale factor and the power law noise amplitude, derived from these long time series, were then used to propagate rates and uncertainties for the shorter time series, for which CATS cannot produce reliable estimates. For the propagation, the time series with fewer than 2000 epochs are additionally subdivided into two categories; continuous sites (≥ 2.5 yr), for which periodic parameters are estimated in the propagation of uncertainties, and very short continuous sites (< 2.5 yr) and campaign sites for which periodic parameters are not estimated. For each campaign, 1 mm of noise was added when propagating the uncertainties, to allow for tiny differences when re-setting up equipment.

Finally, for each site, the uplift rate y^u and its uncertainty σ^u are assessed by manually removing portions of the time series (for example deleting campaigns in turn). If the rate changes by an amount larger than the propagated uncertainty for the site, the uncertainty is assigned as ± the maximum difference in rate, and the rate is adjusted, if necessary, to the values of the most likely part of the range. Sites with only two campaigns were assigned an uncertainty of ± 100 mm/yr, unless there was further evidence for or against the existence of systematic

Earth Syst. Sci. Data Discuss., https://doi.org/10.5194/essd-2017-46
Manuscript under review for journal Earth Syst. Sci. Data
Discussion started: 15 June 2017

errors.

Table 1 summarizes the rate estimation methods and the number of sites for each. For further details and full information on individual rates and time series, see Petrie et al. (in prep a) for a full description of the processing and ensemble evaluation, and Petrie et al. (in prep b) for details of time series analysis and rate and uncertainty estimation. ~~Table 1 shows the numbers of sites at which each approach was taken.~~ Further work was undertaken to combine or 'cluster' the rates regionally for inclusion in the estimation process – see the REGINA Paper II (Sasgen et al. *submitted.)* for details.

(repeats)

Earth Syst. Sci. Data Discuss., https://doi.org/10.5194/essd-2017-46
Manuscript under review for journal Earth Syst. Sci. Data
Discussion started: 15 June 2017

Earth System Science Data
Open Access Discussions

Table 1: Number of sites for each GPS uplift rate and uncertainty estimation method.

Rate and uncertainty estimation method	Number of sites (118 total)
CATS rate and uncertainty ('cats, cats')	18
CATS rate, manually increased uncertainty ('cats, eman')	2
Propagated rate and uncertainty ('prop, prop')	28
Propagated rate and manually increased uncertainty ('prop, eman')	50
Manually adjusted rate and manually increased uncertainty ('rman, eman')	20

Table 2. Uplift rates y^u and associated uncertainties σ^u (mm/yr) for selected GPS sites with more than 2000 epochs of data, compared to data published by Thomas et al. (2011) and Argus et al. (2014). Temporal components and noise characteristics are derived using the CATS software (Williams 2008), i.e. 'cats, cats' method.

frame difference corrected for, or not?

Site	REGINA		Thomas et al. (2011)		Argus et al. (2014)	
	y^u	σ^u	y^u	σ^u	y^u	σ^u
cas1	**1.5**	0.2	**1.2**	0.4	**1.7**	0.8
crar	**0.7**	0.4	**1.0**	0.7	**1.0**	0.6
dum1	**-0.3**	0.3	**-0.8**	0.5	**–0.2**	0.8
maw1	**-0.4**	0.2	**0.1**	0.4	**0.2**	0.6
mcm4	**0.8**	0.2	**0.7**	0.4		
sctb	**0.9**	0.5	**0.6**	1.1		
syog	**1.1**	0.2	**2.3**	0.4	**0.6**	0.8
tnb1	**0.1**	0.5	**-0.2**	0.8	**–0.4**	1.0
vesl	**0.4**	0.3	**1.1**	0.5	**1.5**	0.8
McMurdo*					**1.0**	0.6

*Sites: crar-sctb-mcm4-mcmd

303

3.1 *Comparison with existing results*

Next, we briefly compare the uplift rates at individual sites (data span 1995.0-2013.7)

Earth Syst. Sci. Data Discuss., https://doi.org/10.5194/essd-2017-46
Manuscript under review for journal Earth Syst. Sci. Data
Discussion started: 15 June 2017

Open Access Earth System Science Data Discussions

306 derived from the GPS processing described above with those available from three previous studies: Thomas et al. (2011) (data span 1995.0-2011.0), Argus et al. (2014) (data span 1994-2012) and the more geographically limited set of Wolstencroft et al. (2015) (data span 2006-
309 late 2013, focused on Palmer Land). It should be noted that the REGINA and Wolstencroft et al. (2015) rates are in ITRF2008, the Thomas et al. (2011) rates are in ITRF2005 (which has negligible scale or translation differences to ITRF2008), and the Argus et al. (2014) rates are in
312 a reference frame specific to the paper which they note yields 0.5 mm/yr more uplift than ITRF2008 at high southern latitudes.

Due to the large number of Antarctic sites, in total 118, we focus the comparison on the

Table 3. Uplift rates y^u and associated uncertainties σ^u (mm/yr) for selected GPS sites with fewer than 2000 epochs for data, compared to data published by Thomas et al. (2011) and Argus et al. (2014). Noise characteristics are derived median values from CATS software results for longer station records and propagated in the parameter estimation ('prop, prop' method). See Appendix A.4, Table A.2 for a full list of rates from this study.

Site	REGINA		Thomas et al. (2011)		Argus et al. (2014)	
	y^u	σ^u	y^u	σ^u	y^u	σ^u
belg	**-1.4**	0.7	**3.0**	1.5	**0.8**	2.4
dupt	**11.5**	1.1			**12.4**	2.5
fonp	**13.5**	1.8			**14.8**	3.4
frei	**-4.4**	0.7			**-2.9**	1.4
hugo	**0.9**	1.3			**1.7**	3.6
robi	**8.7**	1.5			**8.7**	3.2
roth	**5.5**	1.4			**5.4**	1.4
svea	**1.3**	1.1	**2.1**	2.0	**1.7**	2.9
vnad	**4.4**	1.1			**5.2**	2.5

frame difference corrected for, or not?

Earth Syst. Sci. Data Discuss., https://doi.org/10.5194/essd-2017-46
Manuscript under review for journal Earth Syst. Sci. Data
Discussion started: 15 June 2017

Open Access Earth System Science Data Discussions

et al. (2014) value (15.0 ± 4.2 mm/yr). Interestingly, the Wolstencroft et al. (2015) rate values for bean, gmez, lntk, mkib, and trve are all systematically higher than the REGINA values, by an average of just over 3 mm/yr, and the uncertainties we assigned are also several times larger. For more detailed analysis of rates and time series at individual sites, see Petrie et al. (in prep b).

Table 4. Uplift rates y^u and associated uncertainties σ^u (mm/yr) for selected sites where uplift rates are manually evaluated based on the spread of rates obtained by sub-sampling the time series ('rman' method), compared to data published by Thomas et al. (2011), Argus et al. (2014), Wolstencroft et al. (2015). See also 'rman' sites in Table Appendix A.4, Table A.2.

Site	REGINA		Thomas et al. (2011)		Argus et al. (2014)		Wolstencroft et al. (2015)	
	y^u	σ^u	y^u	σ^u	y^u	σ^u	y^u	σ^u
bren	**3.1**	1.1	**3.9**	1.6	**2.1**	3.7	**3.2**	0.8
capf	**4.0**	1.4			**15.0**	4.2		
dav1	**-1.6**	0.6	**-0.9**	0.5	**–0.8**	1.0		
mait	**0.4**	1.1	**0.1**	0.6	**1.3**	0.7		
mbl3	**1.3**	17.9	**0.1**	2.0				
bean	**2.1**	4.3					**7.5**	1.2
gmez	**1.5**	4.8					**5.7**	0.8
lntk	**4.6**	3.1					**6.0**	0.7
mkib	**4.7**	2.6					**6.9**	0.5
trve	**2.5**	5.6					**4.7**	0.6

frame difference corrected, or not?

Earth Syst. Sci. Data Discuss., https://doi.org/10.5194/essd-2017-46
Manuscript under review for journal Earth Syst. Sci. Data
Discussion started: 15 June 2017

Open Access Earth System Science Data Discussions

3.2.3 *GPS time series*

The GPS time series were created as part of the RATES project, not solely the REGINA study. They will be made available along with the detailed descriptions in Petrie at al. (in prep b). The time series of vertical bedrock displacement will then be accessible here: [LINK].

Missing Link

4. GRAVIMETRY DATA ANALYSIS

We investigate the Release 5 (RL05) GRACE coefficients of the Centre for Space Research (CSR; Bettadpur, 2012) and the German Research Centre for Geosciences (GFZ; Dahle, 2013), provided up to spherical-harmonic degree and order j_{max}=96 and 90 respectively in the Science Data System (SDS). For reasons of comparison, we adopt j_{max}=90 for both GRACE solutions. A temporal linear trend in the ocean bottom pressure variations modeled by the atmospheric and oceanic background models (GAD) was re-added to the monthly solutions, according the GRACE Science and Data System recommendation (Dobslaw et al. 2013). The GRACE coefficients C_{20} were replaced by estimates from Satellite Laser Ranging (SLR) provided by Cheng et al. (2013). In our analysis we apply the cut-off degrees j_{max}=50, which has been commonly used, as well as $j_{max} = 90$, which is considered experimental in terms of the remaining signal content.

The determination of the rate of the gravity field change over Antarctica follows the scheme sketched in Fig. 3. The rate of the gravity field change, expressed as equivalent water height variations, is estimated in the spatial domain by adjusting a six-parameter function consisting of a constant, a temporal linear trend and annual and semi-annual harmonic amplitudes. A quadratic term was not co-estimated due to the project's focus on the rates (i.e. temporal linear trends). It should be stated that including a quadratic term would slightly reduce the residual uncertainties, particularly in the Amundsen Sea Sector, where an acceleration of mass balance

Earth Syst. Sci. Data Discuss., https://doi.org/10.5194/essd-2017-46
Manuscript under review for journal Earth Syst. Sci. Data
Discussion started: 15 June 2017

4.1 *Optimization of de-striping filter*

The Swenson filter has been proven to effectively reduce the typical north-south correlated error structures of GRACE monthly solutions. The filter is based on the observation that these structures correspond to correlated patterns in the spherical harmonic domain, namely correlations within the coefficients of the same order and even degree, or respectively, odd degree (Swenson & Wahr, 2006). The standard way of fitting and removing these patterns is by adjusting polynomials to the respective sequences of spherical harmonic coefficients, independently for individual months. Parameters to choose are the degree of the polynomial n_{pol} and the minimum order m_{start} starting from which this procedure is applied. In principle, a higher degree polynomial reduces the variability of coefficients of even / odd degree, and results, also at lower minimum order, in stronger filtering – however, the behavior of the filter may differ for regional applications, as discussed below. Note that tuning of other parameters has been presented, e.g. the window width (Duan et al. 2009) or the degree range to which the filter is applied. Chambers and Bonin (2012) have assessed these parameter options with regard to the new GRACE RL05 solutions and global oceanic signals. Here, we perform a detailed analysis of the choice of the Swenson filter parameters in order to optimize the signal-to-noise characteristics of the rate of the gravity-field change over Antarctica. The resulting gravity field rates are later used in the joint inversion for present-day ice-mass change and GIA described in REGINA Part II.

We assess signal corruption by applying the filter to a synthetic test signal, which is based on high-resolution elevation rates from satellite altimetry and reflects the prevailing signatures of present-day ice-change with sufficient realism. For each choice of filter parameters, the signal corruption is assessed as the RMS difference between the original and the filtered

Earth Syst. Sci. Data Discuss., https://doi.org/10.5194/essd-2017-46
Manuscript under review for journal Earth Syst. Sci. Data
Discussion started: 15 June 2017

Open Access Earth System Science Data Discussions

474 comparison it is stated that Chambers & Bonin, 2012 found $m_{start} = 15$ and $n_{pol} = 4$ to be optimal for oceanic applications.

4.2 *Reduction of interannual mass variations*

477 Interannual variations are a major constituent of the temporal variations of the Antarctic gravity field (Wouters et al. 2014). A large portion of the non-linear signal in geodetic mass and volume time series is well explained by modelled SMB fluctuations (Sasgen et al. 2010; 480 Horwath et al. 2012). Towards the ultimate goal of isolating the linear GIA signal from time series of mass change, we removed non-linear effects of modelled SMB variations from the GRACE time series; for this we calculate the *monthly cumulative SMB anomalies* with respect 483 to the time period 1979 to 2012 obtained from RACMO2/ANT (Lenaerts et al. 2012).

We then transfer the monthly cumulative SMB anomalies in terms of their water-equivalent height change into the spherical harmonic domain and subtract them from the monthly GRACE 486 coefficients. In principle, the reduction of the SMB variations from the GRACE time interval has two effects: first, it may change the overall gravity field rate derived from GRACE, depending on the assumption of the SMB reference period. Ideally, the reference period reflects 489 a state of the ice sheet in which input by SMB equals the outflow by ice discharge, and SMB anomalies estimated for today reflect the SMB component of the mass imbalance. However, any bias in the SMB in the reference period leads to an artificial trend in the ice sheet mass 492 balance attributed to SMB. This is an undesired effect, and to avoid it we de-trend the cumulative SMB time series for the time interval coeval to the GRACE analysis (February 2003 to October 2009), before subtracting it from the gravity field rates derived from GRACE (zero 495 difference for *Step 2*, Fig. 3). The second effect is the reduction of the post-fit RMS residual for this known temporal signal variation. After reducing the SMB variations, the propagated RMS

Earth Syst. Sci. Data Discuss., https://doi.org/10.5194/essd-2017-46
Manuscript under review for journal Earth Syst. Sci. Data
Discussion started: 15 June 2017

Open Access Earth System Science Data Discussions

516 4.4 *Gravity field rate and uncertainty assessment*

Fig. 6 shows the estimated RMS uncertainty of the gravity field rate over Antarctica, after post-processing. It is evident that the largest uncertainties are located in a ring south of $-80°$S
519 latitude. This is explained by the design of the Swenson filter; little or no noise reduction is achieved close to the poles, as the gravity field is represented by near-zonal coefficients, which

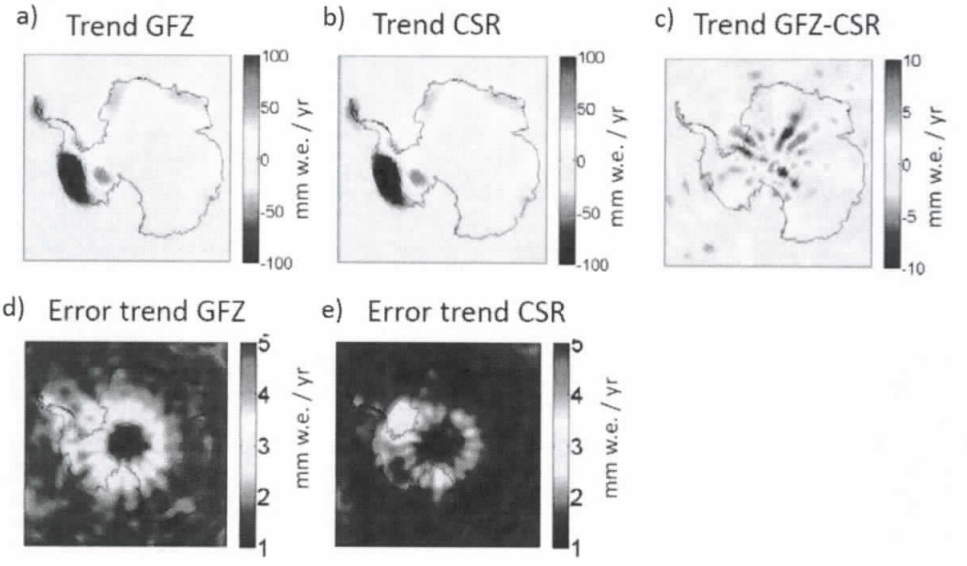

Figure 6. Linear trend in the GRACE gravity fields for the years 2003-2009; a) GFZ RL05a, b) CSR RL05, c) difference between rates from GFZ RL05 and CSR RL05, propagated d) RMS uncertainty for GFZ RL05a and e) RMS uncertainty for CSR RL05.

pass the filter mostly unchanged ($m_{start} = 12$). ~~It is observed that~~ extending the kernel of the
522 Swenson filter to these near-zonal coefficients ($m_{start} \leq 10$) creates high signal corruption and is not suitable for the optimal rate estimate over Antarctica (see Section 4.1). Larger uncertainties are also estimated for the Ronne and Ross ice shelf areas, which are most likely a
525 consequence of incomplete removal of the ocean tide signal during the GRACE de-aliasing

Earth Syst. Sci. Data Discuss., https://doi.org/10.5194/essd-2017-46
Manuscript under review for journal Earth Syst. Sci. Data
Discussion started: 15 June 2017

procedure (Dobslaw et al. 2013). It should also be stated that the RMS uncertainty estimate does not include possible systematic errors in the GRACE solutions, e.g. due to a long-term drift behavior of the observing system.

4.5 *Selection of GRACE release*

Our evaluation of the monthly GRACE uncertainties (Fig. 5), as well as the propagated RMS uncertainty of the temporal linear trend (Fig. 6) indicates that the lowest noise level for the Antarctic gravity field rate (February 2003 to October 2009) is currently achieved with GRACE coefficients of CSR RL05, expanded $j_{max} = 50$. We therefore refrain from including coefficients with $j_{max} > 50$ in order not to ~~comprise~~ compromise the rate estimates by unnecessarily increasing the noise level (see Appendix A.5, Fig. A.3). We adopt CSR RL05 with $j_{max} = 50$ as our preferred solutions for the representation of the gravity field rates over Antarctica, even though GFZ RL05 with $j_{max} = 50$ yields very similar rates (Fig. 6). This choice is supported by the joint inversion, as CSR RL05 with $j_{max} = 50$ provides the highest level of consistency (lowest residual misfit) with the altimetry and GPS data sets (see REGINA Part II, Sasgen et al. 2013, Supplementary Information, Section S.3), which we interpret ~~as~~ to indicate a minimum of spurious signals in the trends. To account for the uncertainty related to our choice of the solution, we consider not only RMS uncertainties of the GRACE rates but also solution differences, in the uncertainty of the final GIA estimate (Fig. 6). The solution difference represent the absolute deviation between trends from GFZ RL05 and CSR RL05 (February 2003 to October 2009, cut-off degree $j_{max} = 50$). These are then summed up squared with the propagated RMS uncertainties. It is acknowledged that the solution differences contain systematic noise arising from the GRACE processing; the pattern and magnitude may change over time. However, they provide a measure how much the results will change, if a GRACE release alternative to CSR

Earth Syst. Sci. Data Discuss., https://doi.org/10.5194/essd-2017-46
Manuscript under review for journal Earth Syst. Sci. Data
Discussion started: 15 June 2017

549 RL05 is considered. The difference between GRACE rates filtered with Gaussian smoothing of 200 km and the optimized Swenson filter together with Gaussian smoothing of 200 km is shown in the Appendix A.5, Fig. A.4.

552 4.6 *Data availability*

4.6.1 *Stokes coefficients of gravity field change*

The monthly GRACE gravity field solutions from the Data System Centers GFZ and CSR 555 are available under ftp://podaac.jpl.nasa.gov/allData/grace/L2/ or http://isdc.gfz-potsdam.de/ as spherical harmonic (SH) expansion coefficients of the gravitations potential (Stokes confidents). More information is available in Bettadpur (2012). The data archive contains 558 temporal linear trends of the fully normalized Stokes coefficients in the 'geodetic norm' (Heiskanen & Moritz, 1967), complete to degree and order 90, inferred from these time series according to Section 4. We provide data for GFZ RL05 and CSR RL05, for the time period 561 2003-2009 and 2003-2013, and for various combinations of filtering. The coefficients are organized as:

[Degree j], [Order m], [c_jm], [s_jm]

564 4.6.2 *Code for de-striping filtering*

The Matlab® function "KFF_filt" performs decorrelation filtering for sets of spherical harmonic coefficients, typically from GRACE gravity field solutions, after the idea of Swenson 567 & Wahr (2006). An open-source alternative to Matlab® is GNU Octave https://www.gnu.org/software/octave/. The function is called as KFF_filt = swenson_filter_2(KFF, ord_min, deg_poly, factorvec, maxdeg), where variables ord_min and 570 deg_poly equal m_{start} and n_{pol}, respectively, in Section 4. KFF contains the sets of spherical harmonic coefficients in the 'triangular' format (not memory-efficient but intuitive). For

Earth Syst. Sci. Data Discuss., https://doi.org/10.5194/essd-2017-46
Manuscript under review for journal Earth Syst. Sci. Data
Discussion started: 15 June 2017

example, for a set of coefficients with maximum degree $j_{max} = 3$ and maximum order $m_{max} = 3$, the set of coefficients is stored in a $j_{max} \times m_{max}$ matrix in the following way:

```
% KFF = [0   0   0   c_00 0   0   0;
%        0   0   s_11 c_10 c_11 0   0;
%        0   s_22 s_21 c_20 c_21 c_22 0;
%        s_33 s_32 s_31 c_30 c_31 c_32 c_33]
```

5. VISCOELASTIC MODELLING

The Earth structure of Antarctica is characterized by a strong dichotomy between east and west, separated along the Transantarctic Mountains (e.g. Morelli & Danesi, 2004). Recent seismic studies have produced refined maps of crustal thicknesses also showing slower upper-mantle seismic velocities in West Antarctica, indicating a thin elastic lithosphere and reduced mantle viscosity (An et al. 2015; Heeszel et al. 2016). Moreover, yield strength envelopes of the Earth's crust and mantle suggest the possibility of a viscously deforming layer (DL) in the lower part of the crustal lithosphere (Ranalli & Murphy, 1987), a few tens of km thick and with viscosities as low as 10^{17} Pa s (Schotman et al., 2008). High geothermal heat flux is in agreement with the seismic inferences of a thin elastic lithosphere and low mantle viscosity, and would favor the presence of such a DL also in West Antarctica (Shapiro & Ritzwoller 2004; Schroeder et al. 2014).

The choice of the viscoelastic modelling approach used to determine load-induced surface displacements and gravitational perturbations is governed by three main requirements; i) to accommodate lateral variations in Earth viscosity, ii) to allow for Earth structures with thin elastic lithosphere and low viscosity layers, in particular including a DL, and iii) to provide

Earth Syst. Sci. Data Discuss., https://doi.org/10.5194/essd-2017-46
Manuscript under review for journal Earth Syst. Sci. Data
Discussion started: 15 June 2017

viscoelastic response functions for the joint inversion of the satellite data described in REGINA paper II (Sasgen et al. *submitted*). To meet these requirements, we adopt the time-domain approach (Martinec 2000) for calculating viscoelastic response functions of a Maxell continuum to the forcing exerted by normalized disc-loads of constant radius. Then, the magnitudes and spatial distribution of the surface loads are adjusted according to the satellite data to obtain the full GIA signal for Antarctica. The forward modelling of viscoelastic response functions a classic topic in sold Earth modelling (e.g. Peltier & Andrews, 1976), however, their application to inverting multiple-satellite observations for present and past ice sheet mass changes is new and applicable to other regions, such as Greenland or Alaska.

The viscoelastic response function approach allows for high spatial resolution at low computational cost in the numerical discretization of the Earth structure as well as in the representation of the load and the response. In addition, we can accommodate a high temporal resolution, which is required when considering low viscosities and associated relaxation times of only a few decades. The spherical harmonic cut-off degree for the simulations shown in the following is $j_{max} = 2048$ (ca. 10 km).

5.1 *Load model parameters*

The load function $\sigma(t, \vartheta)$ is disc shaped with a constant radius of ca. 63 km. The radius of 63 km matches the mean radius of the discs south of 60°S of the geodesic grid (here, ICON 1.2 grid, status 2007, e.g. Wan et al., 2013), which underlie the joint inversion of the altimetry, gravimetry and GPS observations (see REGINA paper II, Sasgen et al. *submitted*.). The resolution of the geodesic grid is chosen to allow for an adequate representation of the load and viscoelastic response with regard to the input data sets, while minimizing the computational cost. The disc load experiment consists of a linear increase in the ice thickness at a rate of 0.5

Earth Syst. Sci. Data Discuss., https://doi.org/10.5194/essd-2017-46
Manuscript under review for journal Earth Syst. Sci. Data
Discussion started: 15 June 2017

Open Access Earth System Science Data Discussions

Is $\dot{\sigma}$ always constant? or constant until dynamic equilibrium, then $\dot{\sigma}=0$?

618 m/yr continuing until a new dynamic equilibrium state between load and response is reached. With reference to the assumed ice density of 910 kg/m³, this thickness increase corresponds to a mass gain of *ca.* 5.6 Gt/yr. Then, to obtain the signal component of the viscous Earth response 621 only, the elastic response and the direct gravitational attraction of the load are subtracted.

The experiment is designed as an *increasing* load, for example representative for the ceasing motion of the Kamb Ice Stream (Ice Stream C; Retzlaff & Bentley, 1993), West 624 Antarctica. Due to linearity of the viscoelastic field equations, it is not necessary to calculate separately the equivalent *unloading* experiment, $-\sigma(t,\vartheta)$, for example corresponding to the past and present glacier retreat of the Amundsen Sea Sector, West Antarctica (Bentley et al. 627 2014 and Rignot et al. 2014, respectively). Among others, the combined inversion of the altimetry, gravity and GPS data (REGINA paper II, Sasgen et al. *submitted.*) solves for the magnitude and the sign of the load, allowing for ice advance as well as ice retreat.

630 5.2 *Earth model parameters*

We set up an ensemble of 58 simulations representing different parameterizations of the viscosity structure (Table 5), split into West Antarctica (56 simulations) and East Antarctica (2 633 simulations). For West Antarctica, varied parameters are the lithosphere thickness, h_L (30 to 90 km in steps of 10 km), the asthenosphere viscosity (1×10^{18} Pa s to 3×10^{19} Pa s in four steps), and the presence of a ductile lower crust, DL, with 10^{18} Pa s. For East Antarctica, we 636 employ parameter combinations appropriate for its cratonic origin with h_L of 150 km and 200 km, and an asthenosphere viscosity equivalent to the upper-mantle viscosity of 5×10^{20} Pa s. These values lie in the range of previously applied viscosity values in Antarctica (Nield et al. 639 2012; Whitehouse et al., 2012; Ivins et al., 2013; van der Wal et al., 2015). For the radial layering of the elastic properties, we adopt the Preliminary Reference Earth Model (PREM;

Earth Syst. Sci. Data Discuss., https://doi.org/10.5194/essd-2017-46
Manuscript under review for journal Earth Syst. Sci. Data
Discussion started: 15 June 2017

thickness of the elastic lithosphere. Note that the Earth response in the equilibrium state only
648 depends on the lithosphere thickness (independent of viscosity), which is therefore consider as the main Earth model parameters in the joint inversion. Further details are presented in REGINA paper II, Sasgen et al. *submitted.*

651 5.3 *Gravity and displacement rate response functions*

The calculated response functions for surface deformation (radial displacement) and gravity (geoid height change) are discretized along 1507 latitudinal points within the range $0 \leq$
654 $\vartheta \leq 90$. Simulations are typically run over 2 kyr with a temporal resolution of $\Delta t = 10$ yr (plus two time steps with constant load thickness). For East Antarctic parameterizations, the simulation period was extended to 20 kyr due to the higher upper-mantle viscosities and
657 associated slower relaxation. However, note that the ratio of geoid-height change versus radial displacement falls off to 1/e after ca. 2 kyr of simulation (Appendix A.6, Fig. A.5). The forcing expected in central East Antarctica is an increase in accumulation towards present-day
660 conditions after ca. 7 ka BP (van Ommen et al. 2004), justifying also the use of equilibrium kernels for East Antarctica. The time derivatives of the radial displacement $\dot{u}$ and of the geoid height change $\dot{e}$ are calculated with a central difference scheme.

do you mean "by 1/e" ? or that it equals 1/e?

Earth Syst. Sci. Data Discuss., https://doi.org/10.5194/essd-2017-46
Manuscript under review for journal Earth Syst. Sci. Data
Discussion started: 15 June 2017

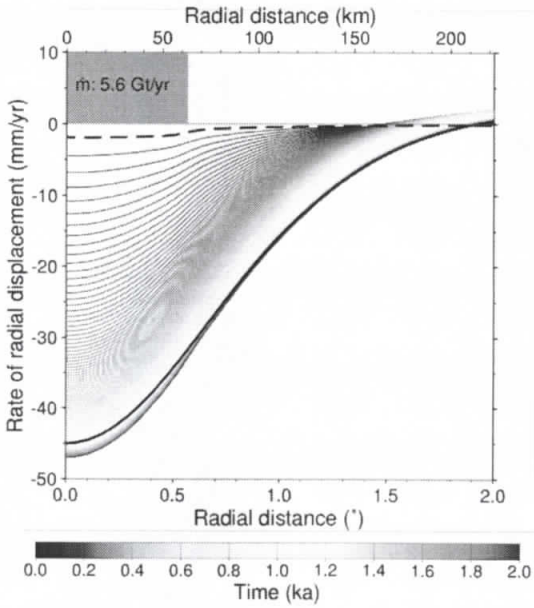

Can you add a panel to these plots showing load(t)? And maybe also $\dot{u}(t, r=0)$?

Figure 7. Displacement rates over the simulation period of 2 kyrs, for an exemplary set of Earth model parameters ($h_L = 30\ km$; $\eta_{AS} = 1 \times 10^{18}\ Pa\ s$). *Shown is the load dimension (grey shading), as well as the instantaneous elastic response (dashed black line) and viscoelastic relaxation only after 2 kyr and no load change (solid black line). The other curves show the rates for the time epoch indicated by the color scale.*

663 Examples of response functions to the loading detailed in Section 5.1 for the rate of radial displacement, $\dot{u}$, and rate of geoid-height change, $\dot{e}$, are shown in Figs 7 and 8, respectively. Instantaneously, the increasing load, $\dot{\sigma}(t) = \text{const.}$, induces an elastic response that is 666 characterized by subsidence and an increase in the direct gravitational potential (dashed lines in Fig. 7 and Fig. 8, respectively). This is the elastic response function adopted in the joint inversion. Note that the elastic response function will not differ between East and West 669 Antarctica, as it is entirely based on the distribution of densities and elastic parameters provided by the PREM. As the load build-up continues, the instantaneous response is followed by the

Earth Syst. Sci. Data Discuss., https://doi.org/10.5194/essd-2017-46
Manuscript under review for journal Earth Syst. Sci. Data
Discussion started: 15 June 2017

777

5.6.3 *Lithosphere thickness*

The thickness of the elastic lithosphere at the locations of the geodesic grid for different
780 values of the viscosity threshold applied to the data set of Priestley & McKenzie, 2013.

lith_thresh_21.disc.txt (threshold 10^{21} Pa s, thicker lithosphere)

lith_thresh_22.disc.txt (threshold 10^{22} Pa s, lithosphere adopted in the GIA estimate)

783 lith_thresh_23.disc.txt (threshold 10^{23} Pa s, thinner lithosphere)

The 1175 entries correspond to the locations of the geodesic grid (Section 5.6.2).

5.6.4 *Open source code for viscoelastic modelling*

786 The open source software package SELEN allows the computation of the Maxwell-viscoelastic Earth response to user-defined ice sheet evolutions, in particular also a simplified disc-load forcing as presented in this paper. The program is downloadable at:
789 https://geodynamics.org/cig/software/selen/

6. Conclusions

In this paper, we have presented refined temporal linear trends of surface elevation, gravity
792 field change and bedrock displacement based on Envisat/ICESat (2003-2009), GRACE (2003-2009) and GPS (1995-2013.7), respectively. In addition, we have performed forward modelling of the viscoelastic response of the solid Earth to a disc-load forcing. These response functions
795 are particularly suited to represent the distinct geological regimes of East and West Antarctica in the joint inversion of multiple satellite data. Similarly, the functions can be applied to the other geographical regions as well. The data and code necessary to reproduce our results, or
798 apply our approach to a different problem, is provide at www.pangea.de, https://doi.pangaea.de/10.1594/PANGAEA.875745.

Earth Syst. Sci. Data Discuss., https://doi.org/10.5194/essd-2017-46
Manuscript under review for journal Earth Syst. Sci. Data
Discussion started: 15 June 2017

Open Access Earth System Science Data Discussions

subsection of this paper (Sections 2 to 5).

AUTHOR CONTRIBUTION

Ingo Sasgen conceived, managed and summarized this study with support of Mark R. Drinkwater. Alba Martín-Español, Bert Wouters and Jonathan L. Bamber performed the altimetry analysis. Alexander Horvath, Martin Horwath and Roland Pail undertook the gravity field analysis, Elizabeth J. Petrie and Peter J. Clarke ~~analysis~~ analyzed and clustered the GPS data with critical input from Terry Wilson. Volker Klemann and Hannes Konrad performed the viscoelastic modelling, with contributions from Ingo Sasgen. All authors were involved in writing and reviewing this manuscript.

Note - at least the data at UNAVCO all (or mostly) have DOIs, either per station or per network.

Table A2 GOOD!

COMPETING INTEREST

The authors declare that they have no conflict of interest.

ACKNOWLEDGEMENTS

The www.regina-science.eu work was enabled through CryoSat+ Cryosphere study funding from the Support To Science Element (STSE) of the European Space Agency (ESA) Earth Observation Envelope Programme. I.S. acknowledges additional funding through the German Academic Exchange Services (DAAD) and DFG grant SA1734/4-1 and P.J.C. and E.J.P. from UK NERC grant NE/I027401/1 (RATES project). We thank Thomas Flament and Frederique Rémy for the Envisat data and Veit Helm for providing the AWI L2 CryoSat-2 re-tracked and corrected elevation measurements. The GPS data used was mainly downloaded from publically available archives. We acknowledge work done by the International GNSS Service (Dow et al., 2009), UNAVCO and the Scientific Committee on Antarctic Research in maintaining such archives, together with the efforts of all the GPS site operators in collecting